sustainability

MDPI

Article

Effect of Hydrothermal Curing on the Hydration and Strength Development of Belite Cement Mortar Containing Industrial Wastes

Dovile Rubinaite, Tadas Dambrauskas *, Kestutis Baltakys and Raimundas Siauciunas

Department of Silicate Technology, Kaunas University of Technology, Radvilenu 19, LT-50270 Kaunas, Lithuania; dovile.rubinaite@ktu.lt (D.R.)

* Correspondence: tadas.dambrauskas@ktu.lt; Tel.: +370-3730-0163; Fax: +370-3730-0152

Abstract: This paper describes the impact of hydrothermal conditions on the strength properties and hydration processes of belite cement mortar samples. The belite-rich binder was synthesized by sintering the initial mixture of raw materials (granite cutting waste, the silica-gel waste from AlF_3 production, and natural materials) in a high-temperature furnace at a temperature of 1150 °C for 2 h. The prepared clinker consists of larnite, mayenite, srebrodolskite, ye'elimite, and gehlenite. To control hydration kinetics and optimize the hardening of belite cement mortar, the produced clinker was blended with 7.5% of gypsum. The mechanical properties were assessed by curing the standard prisms (following the EN 196-1 standard, cement/sand = 1:3, W/C= 0.67) under water-saturated conditions in a stainless steel autoclave. The curing process was performed in a temperature range of 90 °C to 200 °C at various hydrothermal curing durations (6–48 h). The results indicated that the curing conditions highly influence the compressive strength evolution of belite cement mortar and the formed mineralogy of hydrates. The highest compressive strength value (exceeded 20 MPa) was obtained at 200 °C, i.e., when the main belite cement mineral was entirely hydrated and recrystallized into 1.13 nm tobermorite. The microstructural evolution and the phase assemblage during the hydrothermal curing were determined by X-ray diffraction analysis and differential scanning calorimetry.

Keywords: belite cement; hydration; hydrothermal curing; compressive strength; silica-gel waste; granite cutting waste

Citation: Rubinaite, D.; Dambrauskas, T.; Baltakys, K.; Siauciunas, R. Effect of Hydrothermal Curing on the Hydration and Strength Development of Belite Cement Mortar Containing Industrial Wastes. *Sustainability* **2023**, *15*, 9802. https://doi.org/10.3390/su15129802

Academic Editors: Constantin Chalioris and Hosam Saleh

Received: 21 March 2023
Revised: 17 May 2023
Accepted: 14 June 2023
Published: 19 June 2023

1. Introduction

The biggest concern of the 21st century is global warming, which leads to climate change and creates a major threat to life on Earth. According to scientists, this major issue has mainly arisen due to the escalation of greenhouse gases (GHGs) levels [1]. Since the industrial revolution, carbon dioxide (CO_2) accumulation in the atmosphere has increased from ~280 to ~414 ppm. As a result of this increase, CO_2 is one of the most influential gases among the various greenhouse gases and is a direct cause of global warming. Due to such an issue, the European Commission approved The European Green Deal, which aims to avoid dangerous climate change by making Europe a climate-neutral continent by 2050 [2]. In order to implement this policy, transformative actions in various industrial sectors are needed.

As a consequence of industrialization and urbanization, cement manufacturing faces increasing demand every year. Today, the global manufacturing of widely used Ordinary Portland cement (OPC) has reached 4 billion tons per year, and it is anticipated to increase by ~50% by the end of 2050 [3]. Despite its demand, OPC is quite an environmentally controversial material. It is estimated that, on average, the production of 1 ton of OPC clinker releases ~0.87 tons of CO_2 [4]. That includes emissions from the calcination of the raw materials (60–65%) and fuel combustion needed to reach the high-sintering temperature (35–40%). As a result, OPC production corresponds to 6–8% of all artificial carbon

emissions worldwide [5]. At the same time, the manufacture of cement demands extensive amounts of resources and energy. The high calcination temperature (~1450 °C) required to form the main phase of OPC–alite (C_3S) and clinker grinding processes count for about 2–3% of global energy consumption [6]. In addition, around 1.5 tons of starting materials are required to produce 1 ton of OPC [7]. Thus, to implement the EU Green Deal and create a sustainable future, the cement industry must be redesigned by highly focusing on energy savings, reducing clinker factor/quantities of raw materials and significantly cutting CO_2 footprint.

One of the pathways to solving sustainability issues in the cement industry is the broad application of alternative environmentally friendly cement (green types of binders) [8]. A reasonable option to replace OPC may be with types of cement with a high content of belite, i.e., belite calcium sulfoaluminate cement (BCSA), belite-ye'elimite-ferrite cement (BYF), etc. [9,10]. Mentioned types of cement are considered environmentally friendly materials because the formation of the main phase (belite (β-C_2S)) demands less limestone [11]. Therefore, less anthropogenic carbon dioxide is released into the environment during the calcination of the raw materials compared to OPC production. In addition, the required formation energy for belite is lower than that of alite, resulting in a lower furnace operating temperature of approximately 200 °C [12]. For this reason, during the production of belite-rich clinker, not only can the consumption of energy be reduced, but also the carbon footprint from fuel combustion. In addition, the production of these types of cement allows the application of the circular economy model. This model is implemented by replacing traditional raw materials with industrial by-products/wastes. The results of many studies have shown that industrial wastes have a high potential to become alternative raw materials for cement production [13–16].

Depending on the initial design of the raw materials, the mentioned binders may have a quite variable composition that usually contains phases such as ye'elimite ($C_4A_3\hat{S}$), tetracalcium alumino ferrite (C_4AF) and calcium aluminates (C.A., $C_{12}A_7$, and C_3A) [17,18]. Regarding the hydration processes and kinetics of such types of cement, ye'elimite, ferrite, and aluminate phases react during early hydration ages (24 h) and ensure the primary strength of concrete [19]. However, without additives, the reaction of these phases with water is very rapid and can lead to a flash-set phenomenon. Therefore, the other ingredient in such binders typically includes a source of soluble calcium sulphate (gypsum or anhydrite), which assists in regulating hydration kinetics (setting time) and enhances the strength development of concrete. Meanwhile, belite is defined by substantially lower hydraulic activity than mentioned phases and contributes to concrete strength only after 28 days of hydration [20]. The reactivity of belite is an important factor that defines and may limit the application areas of belite-rich cement. One of the possible ways to accelerate the hydration rate of belite can be reached by involving physical activation, i.e., elevating the curing temperature. The steam curing of concrete is a widely used method that can be performed under normal-pressure (below 100 °C) or high-pressure steam [21]. This method is usually beneficial where it is essential to achieve the rapid early strength development of concrete or where additional heat is required to perform hydration. One example is fibre cement products (e.g., board siding) produced by Etex Group (Belgium), whose cement basis constitutes OPC and is manufactured in hydrothermal conditions. Regarding the temperature impact on the hydration of belite-rich cement, in the past, the hydration reaction and strength development mainly focusing on mortar samples cured below 100 °C temperature have been studied [22–25].

In the previous study [26], the mechanical properties of belite cement mortar (also includes ye'elimite, ferrite, and aluminate phases) were examined by curing the standard prisms (following the EN 196-1, cement/sand = 1:3, W/C = 0.67) in an aqueous (20 °C, for 3–90 days) environment. The experiments demonstrated that belite cement mortar samples exhibit slow strength development, i.e., the samples reached only ~10 MPa of compressive strength after 90 days of curing. The main factor responsible for the aforementioned behaviour was the slow hydration rate of the main compound, larnite (belite). The obtained

strength of the cement mortar samples is insufficient to standards and might be a limiting factor in the application of the construction industry. However, as mentioned before, concrete strength development can be efficiently accelerated by introducing additional heat into the cement mortar system and maintaining the required humidity. For this reason, we decided to investigate the hydration behaviour of belite cement by applying the hydrothermal curing method.

This research aims to assess the impact of hydrothermal conditions on the hydration of belite cement mortar mineralogical compounds and strength development. The relationship between formed hydrates and the strength of mortar samples was monitored using instrumental analysis. In order to better understand the potential application of granite cutting waste (GCW) and the AlF_3-rich silica gel waste (which contains up to 10% F^- ions) as starting materials in the production of cementitious binders, the mentioned wastes were used to produce belite-rich cement (with ferrite, aluminate and ye'elimite phases) [27].

2. Materials and Methods

2.1. Raw Materials

The following raw materials were used for the belite clinker production: limestone (purity ~92.86 wt.% of $CaCO_3$, JSC Naujasis kalcitas, Naujoji Akmenė, Lithuania); calcium sulfate hemihydrate ($CaSO_4 \cdot 0.5H_2O$, Knauf, Germany); silica-gel waste, i.e., a waste product of aluminium fluoride production in plant JSC Lifosa (Kėdainiai, Lithuania); granite-cutting waste, i.e., a waste product of granite production in the plant of JSC Granitas (Kaunas, Lithuania); iron (III) oxide (Fe_2O_3, Honeywell, Germany); and aluminium hydroxide ($Al(OH)_3$, Honeywell, Germany); calcium sulphate dihydrate ($CaSO_4 \cdot 2H_2O$, Knauf, Germany). The chemical composition and main characteristics of the raw materials are presented in reference [27].

2.2. Production of Belite Cement

According to the literature [28], belite-rich cement does not have a standardized mineralogical composition. The main criterion covers only the amount of belite in the clinker (>50%). Considering the hydraulic reactivity of the phases, the mineralogical composition of belite clinker was selected: 60% of $2CaO \cdot SiO_2$, 20% of $4CaO \cdot 3Al_2O_3 \cdot SO_3$ and 20% of $4CaO \cdot 3Al_2O_3 \cdot Fe_2O_3$. Based on the identified oxide composition of raw materials and the prospective mineralogical composition of belite clinker, the system of equations was created to estimate the required mix proportions for the initial batch. The composition of the oxides within each compound was considered and aimed that the raw material batch constituting less than 0.04% of F^- ions. Table 1 demonstrates the prospective chemical composition of belite clinker and the calculated mix portions of the initial batch.

To produce the belite clinker (5 kg), the raw materials were weighed and poured into a plastic container (20 L) with five grinding bodies, sealed and homogenized using a laboratory roll ball mill. The homogenization was performed for 1 h at a spinning rate of 120 rpm/min, where grinding bodies were used to ensure homogenization quality. Afterwards, the initial mixture was transferred to a laboratory triangular ball mill, in which 25 grinding bodies were added and ground for 4 h at 60 rpm. This way, the required fineness of the initial mixture was ensured (S_a = 525 m^2/kg). To synthesize the belite clinker, tablets were made and then sintered. For tablet preparation, 500 g of the produced mixture was moisturized with 50 mL of distilled water to ensure the stickiness of the material. Then, the mixture was compressed (10 MPa maintained for 60 s) with a rate of loading of 0.5 MPa/s using square press form (100 × 100 × 40 mm). The prepared tablets (~29 mm in height) were sintered by applying a five-step calcination process in a high-temperature furnace *Nabertherm HTC 03/16*: (1) the temperature was raised to 900 °C by using a 5 °C/min heating rate, (2) maintained for 30 min at 900 °C, and (3) then the temperature was increased from 900 °C to 1150 °C using a 2 °C/min heating rate, (4) where the temperature was maintained at 1150 °C for 2 h; (5) lastly, the tablet was taken out hot (~1000 °C), where simultaneous shredding and (quick) cooling followed. This calcination

method was chosen considering the thermal decarbonation of $CaCO_3$ (800–900 °C) and the characteristic transition of β-C_2S to γ-C_2S within slow cooling. Meanwhile, the sintering temperature of 1150 °C was chosen according to the previous experimental results [27].

Table 1. Prospective mineralogical composition of belite clinker, mixed portions of raw materials, and oxide composition of the used mixtures (excluding H_2O and CO_2).

Prospective Composition, wt.%	
$2CaO{\cdot}SiO_2$	60
$4CaO{\cdot}3Al_2O_3{\cdot}SO_3$	20
$4CaO{\cdot}3Al_2O_3{\cdot}Fe_2O_3$	20
Oxide composition, %	
CaO	55.63
SiO_2	20.93
Al_2O_3	14.23
SO_3	2.62
Fe_2O_3	6.58
Raw material, wt%	
Calcium carbonate	66.67
Hemihydrate gypsum	3.17
Granite cutting waste	14.35
Iron (III) oxide	2.50
Aluminium hydroxide	9.47
Silica gel waste	3.81

The formed belite clinker minerals were identified by XRD and QXRD analysis. It was found that larnite (β-Ca_2SO_4; PDF No. 00-033-0302), mayenite ($C_{12}A_7$)($Ca_{12}Al_{14}O_{33}$, PDF No. 04-014-8824), srebrodolskite (C_2AF) ($Ca_2Mg_{0.1}FeAl_{0.9}O_5$, PDF No. 04-014-9001), magnesium oxide (MgO, PDF No. 00-043-1022), ye'elimite ($C_4A_3\hat{S}$) ($Ca_4Al_6O_{12}SO_4$, PDF No. 00-033-0256), and gehlenite (C_2ASi) ($Ca_2Al_2SiO_7$, PDF No. 00-009-0216) were formed during the sintering. Additionally, the residue of quartz (SiO_2, PDF No. 04-007-0522) was also identified in the sample (Figure 1). It is worth reminding that the added quantity of fluorine in the primary mixture was below 0.04%. Thus, the content of formed compounds with fluorine is too low to identify by XRD analysis. The results of the quantitative analysis showed that the belite clinker consists of 53.5% of belite, 17.4% of mayenite, 15.3% of srebrodolskite, 5.2% of ye'elimite, 4.8% of gehlenite, and 3.8% of other phases. The obtained clinker composition coincides with the expected content of belite and ferrite phases but has a lower ye'elimite quantity. This phenomenon is seen due to the low calcination temperature, where thermal energy is insufficient for solid-state reactions to form ye'elimite. Additionally, the industrial by-product additions induce the formation of complex clinker mineralogy [17]. As a previous study demonstrated [27], the increase in temperature promotes the formation of ye'elimite; however, it adversely affects the stability of larnite (partially β-$C_2S \rightarrow$ γ-C_2S). Thus, regarding the amount of belite in the clinker (>50%), and the hydraulic activity of other formed main phases, the present clinker was used for experimental work. Lastly, the produced clinker was blended with 7.5% of gypsum and milled for 2 h in a ball mill (S_a = 350–400 m^2/kg). The added amount of gypsum is optimal for controlling the belite cement early hydration process, the effect of which has been described in the previous study [26].

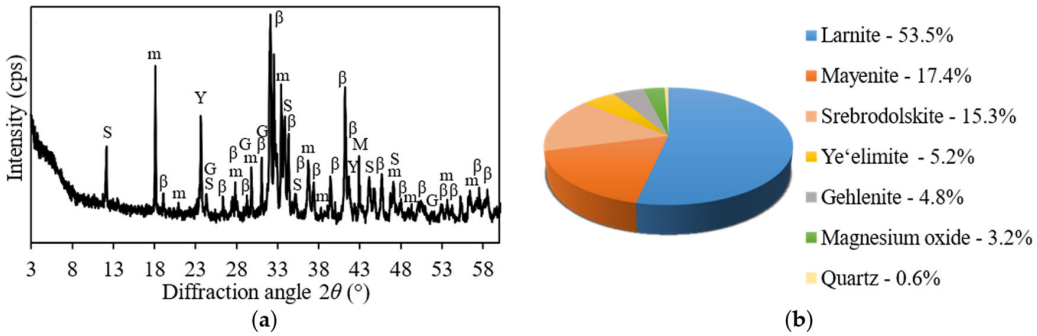

Figure 1. XRD pattern (**a**) and the results of QXRD analysis (**b**) of belite clinker sample. Indexes: β—larnite; m—mayenite; M—magnesium oxide; Y—ye'elimite; S—srebrodolskite; G—gehlenite.

2.3. The Hardening of Samples

The compressive strength test for belite mortar samples was performed according to EN 196-1 and EN 12390-6 standards [29,30]. The standard prisms (40 × 40 × 160 mm) were prepared by mixing the produced belite cement with standard sand (the cement/sand ratio equal to 1:3) and water. Binders with aluminate phases are known to require a higher water-to-solids (W/C) ratio than OPC cement [17]. Thus, the W/C used in this work was 0.67 to ensure proper mortar consistency and workability. The prepared fresh mortar was cast into sealed metal moulds in which the pre-curing at 20 ± 1 °C for 3 h was performed. Afterwards, the pre-cured prism samples were demoulded and transferred into an 18.5 L stainless-steel autoclave ("Parr instruments", model 4621, Moline, IL, USA), in which hydrothermal curing was performed at the temperature range of 90–200 °C for 6–48 h. The selected temperatures were reached using a 25 °C/h heating rate. After hardening, the compressive strength of samples was determined using a press FORM + TEST MEGA 10-400-50 (Riedlingen, Germany) with a rate of loading of 0.05 kN/s for the flexural strength and 2.4 kN/s for the compressive strength. The three samples were tested for each type of cement mortar under all curing conditions. The average of three specimens was used as the compressive strength, where the standard deviation represents the average variability of the results. For the instrumental characterization of hydration products, the samples were crushed to powder, rinsed with propanol (to stop hydration), dried in an oven at 50 ± 0.2 °C for 24 h, and sieved through an 80-μm mesh to ensure particle distribution.

2.4. Analytical Techniques

X-ray diffraction analysis (XRD) was carried out to determine the formed crystal structure changes. The measurements were performed at room temperature with the D8 Advance diffractometer (Bruker AXS GmbH, Karlsruhe, Germany) equipped with a CuKα X-ray tube operated at 40 kV and 45 mA. Diffraction patterns were recorded in the Bragg–Brentano geometry using a fast-counting detector Bruker LynxEye based on silicon strip technology. The measurement range was 2θ = 3–70° with steps of 0.020° 2θ with a time per step of 0.2 s, corresponding to a total measurement duration of ~12 min per sample.

Differential scanning calorimetry (DSC) was carried out to analyse the hydration products using Netzsch Polyma DSC 214 analyser (Netzsch, Germany) with the type E thermocouple. Measurement parameters: temperature heating rate—10 °C/min, temperature range—20–600 °C, the crucible—aluminium (Al) crucible with a lid, the atmosphere in the furnace—nitrogen, measurement accuracy— ±3 °C. The data were assessed with NETZSCH Proteus software Version 7.0.0.

3. Results and Discussion

In the first step of steam curing, the belite cement mortar samples were cured in the temperature range of 90–200 °C, and the exposure duration was 24 h. The influence of the high-temperature exposure effect on the formation of the belite cement hydrates was investigated by XRD and DSC analysis. It was found that after hydrothermal curing at

90 °C temperature, the compressive strength of belite cement mortar samples achieved 3.92 MPa, and a flexural strength of 1.9 MPa (Figure 2).

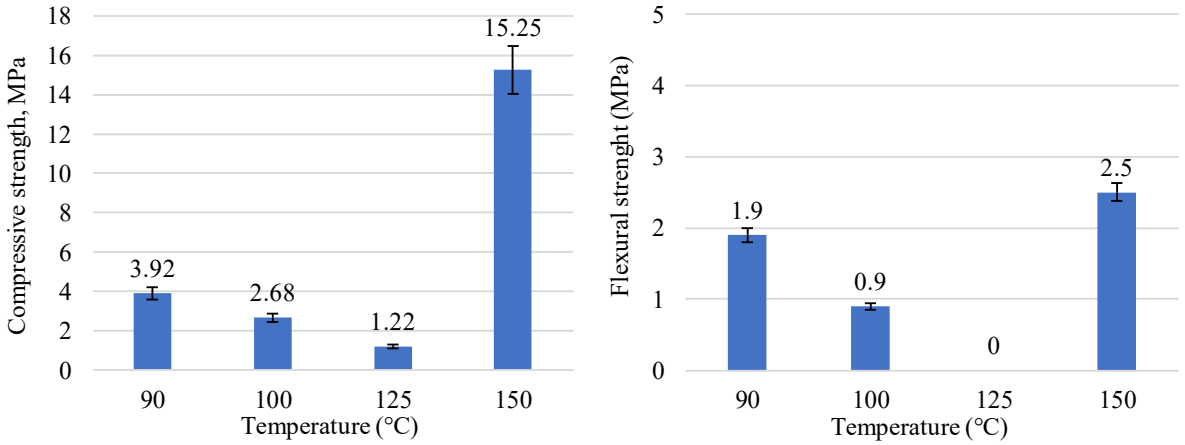

Figure 2. Strength development of belite cement mortar samples cured in the hydrothermal environment at different temperatures with an isothermal time of 24 h (error bars represent standard deviation).

XRD results demonstrated that under these curing conditions, mayenite, gypsum, srebrodolskite, gehlenite and ye'elimite were completely reacted (Figure 3a and Table 2). The diffraction patterns showed that the main formed crystalline phases were calcium aluminium silicate–katoite (C_3AH_6, PDF No. 04-017-1504), calcium aluminium iron hidrosilicate (C_3AFSH_4) ($Ca_3AlFe(SiO_4)(OH)_8$, PDF No. 00-032-0147) and calcium monosulfoaluminate hydrate ($C_4A\hat{S}H_{12}$) ($Ca_4Al_2O_6(SO_4)_{0.5}(O.H.)\cdot 12H_2O$, PDF No. 00-042-0065). Moreover, it is likely that various other hydration products also formed in addition to the mentioned hydrates: hydrogarnet, portlandite, etc. [31,32]. Unfortunately, due to the high intensity of the peaks of quartz and the low content and/or crystallinity of mentioned hydrates, they were not clearly observed in XRD patterns. Additionally, a basal reflection in a 26°–34° diffraction angle range was detected, which is characteristic of calcium silicate hydrate gel (C–S–H gel) [32]. The formation of the compounds mentioned above can be described by these reactions [33–35]:

$$C_2S + 2H \rightarrow CH + C\text{–}S\text{–}H \quad (1)$$

$$C_2S + C_2AF + 5H \rightarrow C_3AFSH_4 + CH \quad (2)$$

$$C_4A_3\hat{S} + 18H \rightarrow C_4A\hat{S}H_{12} + 2AH_3 \quad (3)$$

$$C_{12}A_7 + 27H \rightarrow 4C_3AH_6 + 3AH_3 \quad (4)$$

Table 2. Alterations in the main diffraction peaks characteristic of the initial clinker and hydration products of belite cement mortar samples after hydrothermal curing at different temperatures with an isothermal time of 24 h.

Conditions / Compound	Intensity (cps)			
	90 °C	**100 °C**	**125 °C**	**150 °C**
Larnite (0.279 nm)	389	386	385	343
Katoite (0.505 nm)	311	353	593	561
1.13 tobermorite (1.139 nm)	-	-	-	380
Calcium aluminium iron silicate hydroxide (0.438 nm)	302	346	454	430
Calcite (0.304)	193	197	203	190
Calcium monosulfoaluminate (0.893)	248	142	-	-

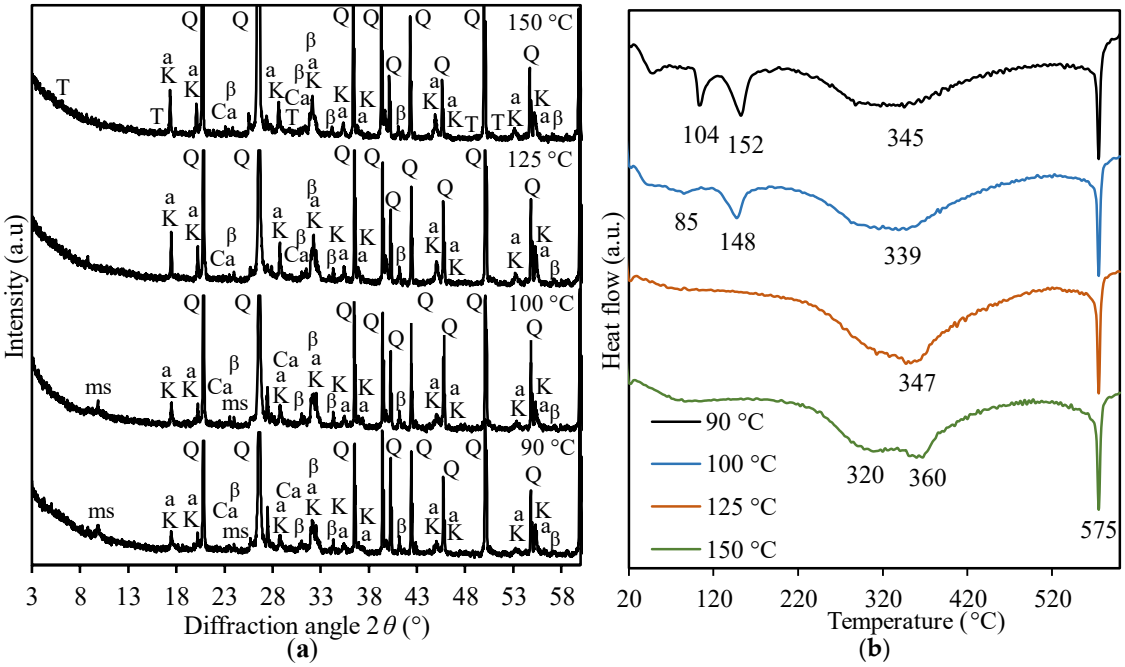

Figure 3. XRD patterns (**a**) and DSC (**b**) curves of belite cement mortar samples after hydrothermal curing. Indexes: β—larnite; Q—quartz; K—katoite; T—1.13 tobermorite; Ca—calcite; a—calcium aluminium iron hydrosilicate; ms—calcium monosulfoaluminate.

It was observed that under these curing conditions, the main belite cement mineral–larnite exhibited a low hydration degree (Figure 3a). Moreover, calcium carbonate ($CaCO_3$, PDF No. 04-012-0489) was observed in the hydration products due to the interaction of the samples with atmospheric carbon dioxide. It is worth mentioning that the available amount of periclase (MgO) in all hydrothermally treated belite cement mortar samples was so low that it was not detected in XRD patterns. For this reason, the hydration activity of periclase under hydrothermal conditions was not investigated in this work. Nevertheless, previous studies demonstrated that elevated temperature accelerates the dissolution of periclase and causes the precipitation of brucite ($Mg(OH)_2$) [36]. Thus, hydration products also might contain a low quantity of brucite.

The results of the X-ray diffraction analysis were supported by differential scanning calorimetry data (Figure 3b). Four endothermic effects were observed in the DSC curve. The first endothermic effect at ~104 °C reflected the elimination of adsorption water, and the dehydration of amorphous ettringite and other amorphous structure compounds [37,38]. The peak observed at higher temperatures (~152 °C) was attributed to the dehydration of calcium monosulfoaluminate. A broad endothermic effect in the temperature range of 200–380 °C can be attributed to the decomposition of amorphous aluminium hydroxide, katoite and hydrogrossulars, while a sharp shoulder at 575 °C characterized the conversion of the quartz α↔β phase [39].

It was determined that raising curing temperatures to 100 °C and 125 °C adversely affected the compressive and flexural strength of the belite cement samples (Figure 2). It was measured that the compressive strength values of belite cement samples reached up to 3 MPa (Figure 2). Based on XRD results, under these curing conditions, higher amounts of katoite and hydrogrossular crystallized (Figure 3a and Table 2). Meanwhile, the diffraction peaks of calcium monosulfoaluminate decreased and were no more detected in XRD patterns. The same transition also was observed in DSC curves. It was determined that after curing samples at 100 °C, the heat flow of the first two endothermic effects decreased from ~14 J/g to 6 J/g, and after curing samples at 125 °C, these endothermic effects were no longer identified (Figure 3b). Moreover, the heat-flow value of the katoite and hydrogrossular dehydration process increased from 34 J/g to 51 J/g at 100 °C and 125 °C, respectively.

This suggests that the contents of katoite and C_3AFSH_4 are inversely proportional to the compressive strength of the sample curing in the temperature range of 90–125 °C.

It should be emphasized that during the pre-curing stage, the main formed hydrate is ettringite (molar volume ~707 cm^3/mol [40]), which ensures binding and gives the initial strength of the sample. Meanwhile, in the hydrothermal treatment stage, ettringite gradually begins to decompose to monosulfoaluminate (above 70 °C) (molar volume ~310 cm^3/mol [41]), which, as results show, disintegrates at 125 °C. These structural transitions probably lead to solid-volume changes and cause reduced compressive strength values of belite cement mortar samples. Unfortunately, there is a lack of information on the curing of belite mortar under hydrothermal conditions in the literature, so this observed phenomenon requires deeper study.

A significant difference in the compressive and flexural strength of belite cement mortar samples was observed at the curing temperature of 150 °C, where the values increased to 15.25 MPa and 2.5 MPa, respectively (Figure 2). It was determined that the increment in compressive strength is related to the crystallization of the new calcium silicate hydrate–1.13 nm tobermorite ($Ca_{2.24}SiO_3O_{7.5}(OH)_{1.5}(H_2O)$, PDF No. 04-011-0270) (Figure 3a and Table 2). Previous studies have also acknowledged that the formation of 1.13 tobermorite determines the strength properties of the concrete products (for instance, autoclaved aerated concrete (AAC)) cured in the environment of saturated water vapour [41]. This behaviour is essentially observed due to the dense structure of this compound. It should be noted that under these curing conditions, the intensity of the diffraction peaks of katoite and calcium aluminium iron hydrosilicate slightly decreased (Figure 3a and Table 2). The DSC data also affirmed the XRD results, where the value of the endothermic effect in the temperature interval of 250–400 °C decreased ~1.5 times (from 51 J/g to 33 J/g). It is worth mentioning that 1.13 nm tobermorite has no specific effect on the DSC curves. These results indicated that the formation of 1.13 nm tobermorite is an essential factor influencing the final strength properties of the cured belite cement stone.

Further temperature increase to 175 °C enhanced the strength properties of belite cement mortar samples to 18.32 MPa compressive strength and 3.3 MPa flexural strength (Figure 4). Moreover, it was determined that a reduction in isothermal time to 12 h negatively impacted the compressive strength values of belite samples, as they decreased about 1.4 times (Figure 4). According to the results of the XRD, the formed amount of crystalline 1.13 tobermorite had the highest impact on the strength properties of the belite cement samples, i.e., after a reduced processing duration, a decreased intensity of the main peak of 1.13 tobermorite was observed (from 455 cps to 394 cps) (Figure 5). It is worth highlighting that under these curing conditions, hydration of larnite significantly accelerated, i.e., the intensity of the diffraction peaks decreased about 70–78% (Figure 5 and Table 3).

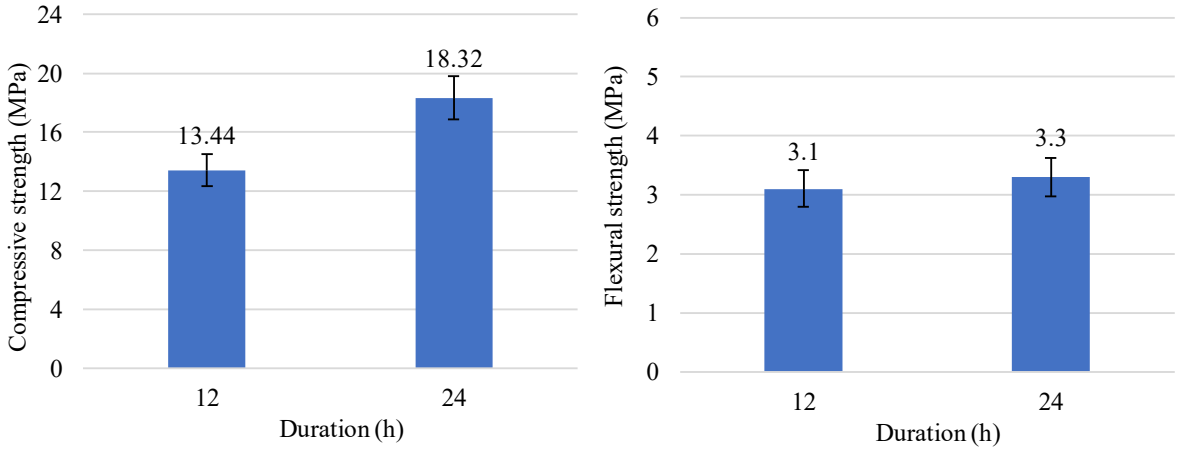

Figure 4. Strength development of belite cement mortar samples cured in the hydrothermal environment at 175 °C (error bars represent standard deviation).

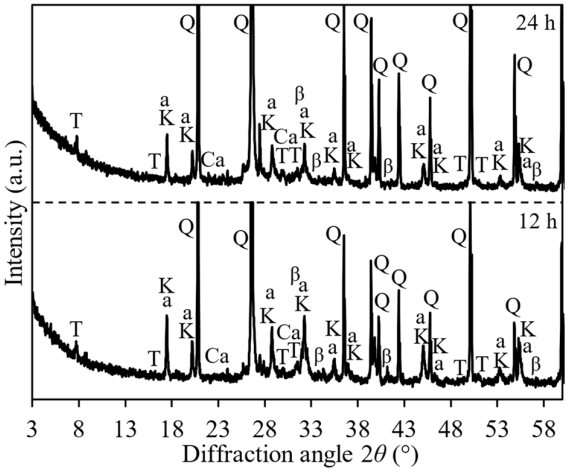

Figure 5. XRD patterns of belite cement mortar samples after hydrothermal curing at 175 °C temperature. Indexes: β—larnite; Q—quartz; K—katoite; T—1.13 tobermorite; Ca—calcite; a—Calcium aluminium iron hydrosilicate.

Table 3. Alterations in the main diffraction peak characteristics of the initial clinker and hydration products of belite cement mortar samples depend on the hydrothermal curing conditions.

Conditions / Compound	Intensity (cps)					
	175 °C 12 h	**175 °C 24 h**	**200 °C 6 h**	**200 °C 12 h**	**200 °C 24 h**	**200 °C 48 h**
Larnite (0.279 nm)	341	245	276	264	-	-
Katoite (0.505 nm)	573	460	519	479	484	462
1.13 tobermorite (1.139 nm)	394	455	423	457	695	557
Calcium aluminium iron hydrosilicate (0.438 nm)	400	345	423	396	438	405
Calcite (0.304)	215	197	207	207	200	219

The highest compressive strength values were obtained when samples were cured at 200 °C for 24 h and reached 20.07 MPa (Figure 6). Meanwhile, a reduced (up to 6 h) or increased (up to 48 h) duration of curing negatively affected the strength properties of belite cement mortar samples. The investigation of the mineral composition of the belite cement samples (cured at 200 °C for 24 h) showed that the main diffraction maximums of katoite and C_3AFSH_4 increased by ~5% and ~21%, respectively, and the intensity of 1.13 tobermorite even increased by ~34% (from 455 cps. to 695 cps.) compared to the samples cured for 24 h at 175 °C. It was observed that, under these curing conditions, the main cement phase-larnite fully recrystallized into the hydration products, i.e., diffraction peaks characteristic of larnite were no longer seen in XRD patterns (Figure 7a and Table 3). Meanwhile, after the reduced duration of curing from 24 h to 12 h or 6 h, the main diffraction peak characteristics of 1.13 nm tobermorite were lower by ~34% and ~39%, respectively. The remaining unreacted larnite was observed in both samples. In addition, it was identified that the intensity of the diffraction peaks of 1.13 tobermorite decreased by extending the duration of hydrothermal curing to 48 h. It suggests that the formed 1.13 tobermorite becomes metastable and partially transforms into other hydration products or amorphous states. Moreover, the intensity of the diffraction peaks of other hydration products was also reduced: katoite ~4.5% and C_3AFSH_4 ~7.5%. These hydrates are likely unstable upon prolonged curing conditions and undergo a phase transition into other compounds that do not exhibit binding properties.

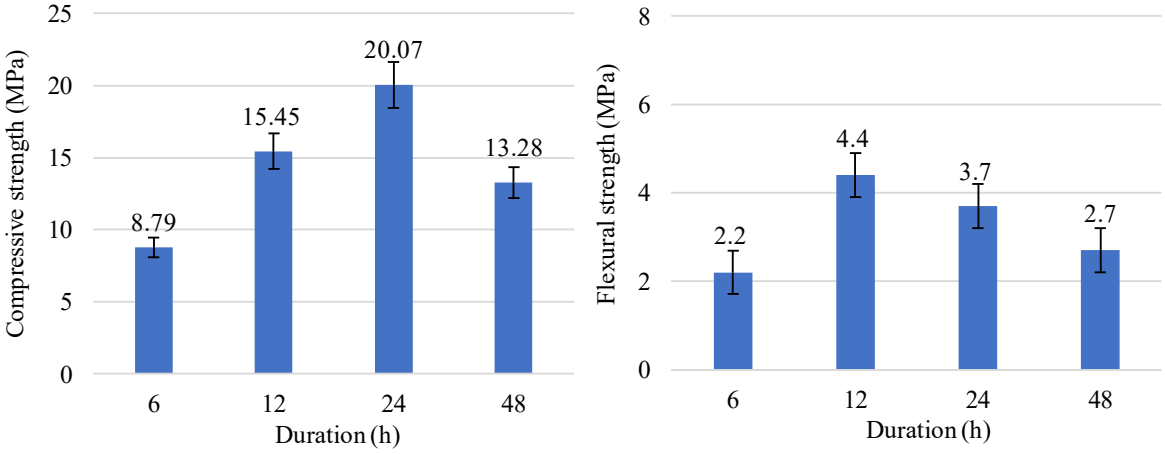

Figure 6. Strength development of belite cement mortar samples cured in the hydrothermal environment at 200 °C (error bars represent standard deviation).

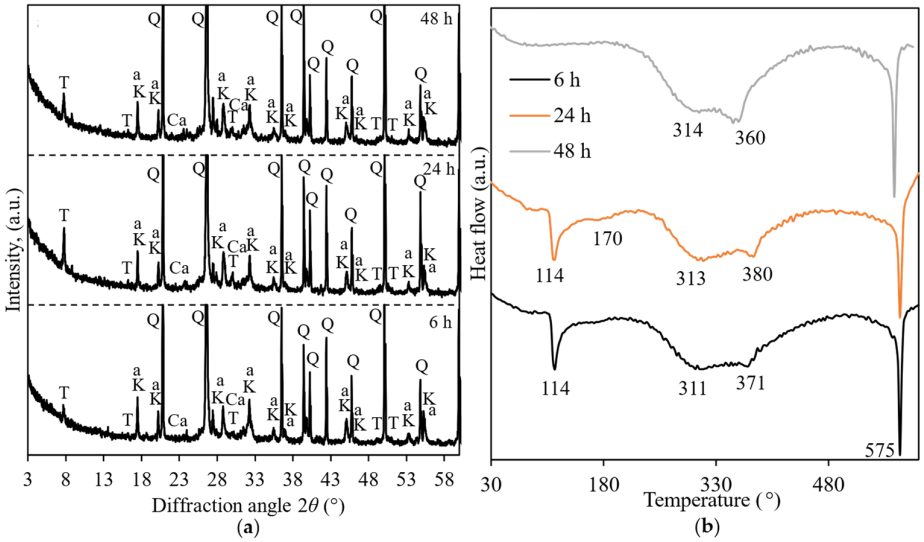

Figure 7. XRD patterns (**a**) and DSC curves (**b**) of belite cement mortar samples after hydrothermal curing at 200 °C. Indexes: β—larnite; Q—quartz; K—katoite; T—1.13 tobermorite; Ca—calcite; a—calcium aluminium iron hydrosilicate.

As evident from the experimental data presented above, the increase in curing temperature promotes the hydration rate of the synthesized belite cement phases, influencing cement-mortar strength properties. The increase in compressive strength is directly related to the hydration of larnite and the formation of 1.13 nm tobermorite. Hydration product development of belite mortar samples cured in the hydrothermal environment at different temperatures with an isothermal time of 24 h is summarised and presented in Figure 8. It is worth mentioning that the obtained compressive strength values of produced belite mortar samples cured for 24 h at 200 °C match the requirements for structural concrete in building special moment frames and special structural walls (ACI 318M-19) and masonry cement class MC5 (EN 413-1).

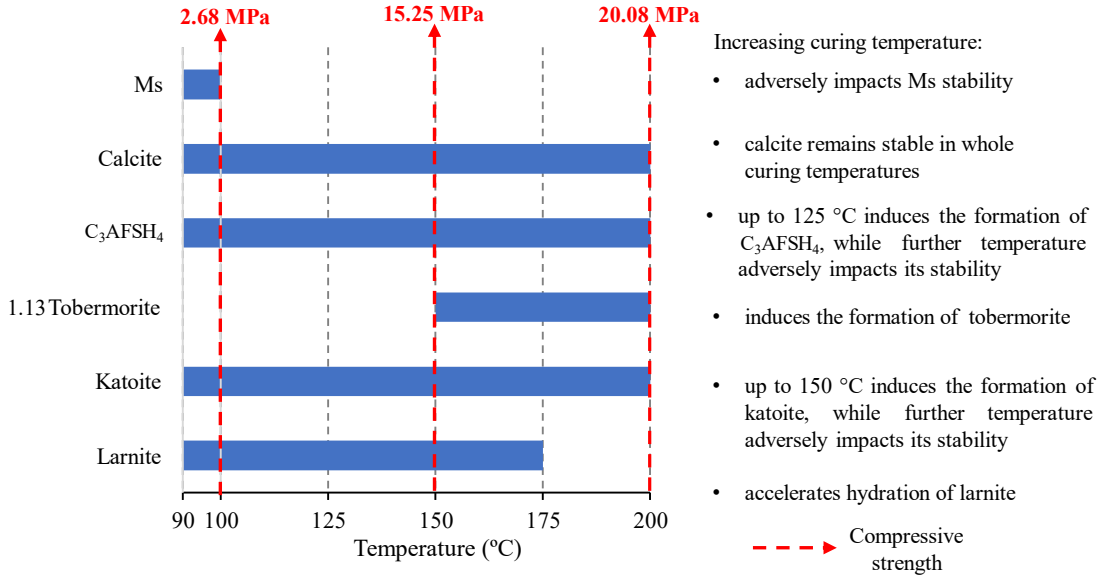

Figure 8. Formation and stability of hydration products of belite cement mortar samples after hydrothermal curing at different temperatures with an isothermal time of 24 h.

Moreover, it is important to understand that even if the experimental results demonstrate the feasibility of alternatively managing industrial waste, the development of this technology requires fundamental changes in the production processes, and the technology itself is very complicated. In order to manufacture this kind of cement on a larger scale, the issues regarding operational and chemical composition standpoints must also be resolved.

4. Conclusions

In this study, the hydration of belite cement and the development of its strength by applying the hydrothermal curing method were investigated. The belite-rich clinker was successfully synthesized when the starting materials consisted of natural raw materials (~82%) and industrial wastes (~18%). The clinkering temperature of 1150 °C for 2 h was sufficient for complete phase formation. The obtained belite clinker consists of 53.5% of β-Ca_2SO_4, 17.4% of $C_{12}A_7$, 15.3% of C_2AF, 5.2% of $C_4A_3\hat{S}$, 4.8% of C_2ASi, and 3.8% of other phases. To ensure optimal hydration behaviour, the belite clinker was blended with 7.5% of gypsum.

The results demonstrated that the elevated curing temperature plays an essential role in the hydration behaviour and the mechanical properties of belite cement. It was investigated that after hydrothermal curing at 90 °C for 24 h, the compressive strength of samples was equal to only 3.92 MPa. With a further curing-temperature increase (up to 125 °C for 24 h), the compressive strength values of the samples were observed to be even lower. Nevertheless, a significant increase in the compressive strength of belite cement mortar samples was determined when samples were cured at ≥150 °C, while the highest value (20.07 MPa) was reached after 24 h of curing at 200 °C.

The results of XRD and DSC confirmed that the identified initial strength properties (at 90 °C) are mainly related to the formation of $C_4A\hat{S}H_{12}$, C_3AH_6 and C_3AFSH_4. Meanwhile, the adverse effects on the compressive strength after curing samples at 125 °C was probably associated with inner solid-volume changes led by the decomposition of calcium monosulfoaluminate. The increment in compressive strength at ≥150 °C was related to the hydration of larnite and the formation of crystalline 1.13 nm tobermorite.

In summary, the results confirmed that hydrothermal curing promotes the hydration of belite cement's main phase-larnite. Accordingly, cement mortar samples cured for 24 h at 200 °C exhibited twice the compressive strength values as samples cured in a water environment after 90 days.

Author Contributions: This paper was written using the contribution of all authors. D.R.: investigation, methodology, validation, visualization, writing; T.D.: data overview, validation, writing—review and editing, supervision; K.B.: conceptualization, supervision, writing—review and editing; R.S.: oversight of the experiment, writing, editing, supervision. All authors have read and agreed to the published version of the manuscript.

Funding: This research was funded by a grant (No. S-MIP-21-4) from the Research Council of Lithuania.

Institutional Review Board Statement: Not applicable.

Informed Consent Statement: Not applicable.

Data Availability Statement: The data presented in this study are available within the manuscript.

Conflicts of Interest: The authors declare no competing interest.

References

1. Pisoft, P.; Sacha, P.; Polvani, L.M.; Añel, J.A.; de La Torre, L.; Eichinger, R.; Foelsche, U.; Huszar, P.; Jacobi, C.; Karlicky, J.; et al. Stratospheric Contraction Caused by Increasing Greenhouse Gases. *Environ. Res. Lett.* **2021**, *16*, 064038. [CrossRef]
2. European Commission. The European Green Deal, Communication from the Commission to the European Parliament, the European Council, the Council, the European Economic and Social Committee of the Regions (COM (2019) 640 Final). 2019. Available online: https://ec.europa.eu/info/sites/default/files/european-green-deal-communication_en.pdf (accessed on 20 November 2022).
3. Andrew, R.M. Global CO_2 Emissions from Cement Production, 1928–2018. *Earth Syst. Sci. Data* **2019**, *11*, 1675–1710. [CrossRef]
4. Schneider, M. The Cement Industry on the Way to a Low-Carbon Future. *Cem. Concr. Res.* **2019**, *124*, 105792. [CrossRef]
5. Wei, J.; Cen, K.; Geng, Y. Evaluation and Mitigation of Cement CO_2 Emissions: Projection of Emission Scenarios toward 2030 in China and Proposal of the Roadmap to a Low-Carbon World by 2050. *Mitig. Adapt. Strateg. Glob. Chang.* **2019**, *24*, 301–328. [CrossRef]
6. Madlool, N.A.; Saidur, R.; Hossain, M.S.; Rahim, N.A. A Critical Review on Energy Use and Savings in the Cement Industries. *Renew. Sustain. Energy Rev.* **2011**, *15*, 2042–2060. [CrossRef]
7. Rahman, A.; Rasul, M.G.; Khan, M.M.K.; Sharma, S. Impact of Alternative Fuels on the Cement Manufacturing Plant Performance: An Overview. *Procedia Eng.* **2013**, *56*, 393–400. [CrossRef]
8. Sivakrishna, A.; Adesina, A.; Awoyera, P.O.; Kumar, K.R. Green Concrete: A Review of Recent Developments. *Mater. Today Proc.* **2020**, *27*, 54–58. [CrossRef]
9. Kotsay, G.; Jaskulski, R. Kotsay and Jaskulski/Belite cement as an ecological alternative to Portland cement—A review. *Mater. Struct. Technol. J.* **2019**, *2*, 70–76. [CrossRef]
10. Gartner, E. Industrially Interesting Approaches to "Low-CO_2" Cements. *Cem. Concr. Res.* **2004**, *34*, 1489–1498. [CrossRef]
11. Naqi, A.; Jang, J.G. Recent Progress in Green Cement Technology Utilising Low-Carbon Emission Fuels and Raw Materials: A Review. *Sustainability* **2019**, *11*, 537. [CrossRef]
12. Biernacki, J.J.; Bullard, J.W.; Sant, G.; Brown, K.; Glasser, F.P.; Jones, S.; Ley, T.; Livingston, R.; Nicoleau, L.; Olek, J.; et al. Cements in the 21st Century: Challenges, Perspectives, and Opportunities. *J. Am. Ceram. Soc.* **2017**, *100*, 2746–2773. [CrossRef]
13. El-Alfi, E.A.; Gado, R.A. Preparation of Calcium Sulfoaluminate-Belite Cement from Marble Sludge Waste. *Constr. Build. Mater.* **2016**, *113*, 764–772. [CrossRef]
14. García-Maté, M.; de La Torre, A.G.; León-Reina, L.; Aranda, M.A.G.; Santacruz, I. Hydration Studies of Calcium Sulfoaluminate Cements Blended with Fly Ash. *Cem. Concr. Res.* **2013**, *54*, 12–20. [CrossRef]
15. Telesca, A.; Matschei, T.; Marroccoli, M. Study of Eco-Friendly Belite-Calcium Sulfoaluminate Cements Obtained from Special Wastes. *Appl. Sci.* **2020**, *10*, 8650. [CrossRef]
16. Gao, Y.; Li, Z.; Zhang, J.; Zhang, Q.; Wang, Y. Synergistic Use of Industrial Solid Wastes to Prepare Belite-Rich Sulphoaluminate Cement and Its Feasibility Use in Repairing Materials. *Constr. Build. Mater.* **2020**, *264*, 120201. [CrossRef]
17. Bullerjahn, F.; Zajac, M.; ben Haha, M. CSA Raw Mix Design: Effect on Clinker Formation and Reactivity. *Mater. Struct. Constr.* **2015**, *48*, 3895–3911. [CrossRef]
18. Morin, V.; Termkhajornkit, P.; Huet, B.; Pham, G. Impact of Quantity of Anhydrite, Water to Binder Ratio, Fineness on Kinetics and Phase Assemblage of Belite-Ye'elimite-Ferrite Cement. *Cem. Concr. Res.* **2017**, *99*, 8–17. [CrossRef]
19. Cadix, A.; James, S. Chapter 5—Cementing Additives. In *Fluid Chemistry, Drilling and Completion*; Wang, Q., Ed.; Oil and Gas Chemistry Management Series; Gulf Professional Publishing: Houston, TX, USA, 2022; Volume 187–254, ISBN 978-0-12-822721-3.
20. Cuesta, A.; Ayuela, A.; Aranda, M.A.G. Belite Cements and Their Activation. *Cem. Concr. Res.* **2021**, *140*, 106319. [CrossRef]
21. Tighare, P.; Singh, M.R.C. Study of Different Methods of Curing of Concrete & Curing Periods. *Int. J. Res. Appl. Sci. Eng. Technol.* **2017**, *5*, 444–447.
22. Borštnar, M.; Lengauer, C.L.; Dolenec, S. Quantitative in Situ X-ray Diffraction Analysis of Early Hydration of Belite-calcium Sulfoaluminate Cement at Various Defined Temperatures. *Minerals* **2021**, *11*, 297. [CrossRef]

23. Xu, L.; Liu, S.; Li, N.; Peng, Y.; Wu, K.; Wang, P. Retardation Effect of Elevated Temperature on the Setting of Calcium Sulfoaluminate Cement Clinker. *Constr. Build. Mater.* **2018**, *178*, 112–119. [CrossRef]
24. Shirani, S.; Cuesta, A.; Morales-Cantero, A.; de la Torre, A.G.; Olbinado, M.P.; Aranda, M.A.G. Influence of Curing Temperature on Belite Cement Hydration: A Comparative Study with Portland Cement. *Cem. Concr. Res.* **2021**, *147*, 106499. [CrossRef]
25. Borštnar, M.; Daneu, N.; Dolenec, S. Phase Development and Hydration Kinetics of Belite-Calcium Sulfoaluminate Cements at Different Curing Temperatures. *Ceram. Int.* **2020**, *46*, 29421–29428. [CrossRef]
26. Rubinaite, D.; Dambrauskas, T.; Baltakys, K.; Siauciunas, R. Investigation on the Hydration and Strength Properties of Belite Cement Mortar Containing Industrial Waste. *J. Therm. Anal. Calorim.* **2022**, *148*, 1481–1490. [CrossRef]
27. Baltakys, K.; Dambrauskas, T.; Rubinaite, D.; Siauciunas, R.; Grineviciene, A. Formation and Hydration of Eco-Friendly Cement Using Industrial Wastes as Raw Materials. *Sci. Rep.* **2021**, *11*, 14742. [CrossRef] [PubMed]
28. Gartner, E.; Sui, T. Alternative Cement Clinkers. *Cem. Concr. Res.* **2018**, *114*, 27–39. [CrossRef]
29. *EN 196-1:2015*; Methods of Testing Cement—Part 1: Determination of Strength. European Committee for Standardization: Brussels, Belgium, 2005.
30. *EN-12390-6:2000*; Testing Hardened Concrete—Part 6: Tensile Splitting Strength of Test Specimens. Beuth Verlag GmbH: Berlin, Germany, 2010.
31. Chen, I.A.; Juenger, M.C.G. Synthesis and Hydration of Calcium Sulfoaluminate-Belite Cements with Varied Phase Compositions. *J. Mater. Sci.* **2011**, *46*, 2568–2577. [CrossRef]
32. Rungchet, A.; Chindaprasirt, P.; Wansom, S.; Pimraksa, K. Hydrothermal Synthesis of Calcium Sulfoaluminate-Belite Cement from Industrial Waste Materials. *J. Clean. Prod.* **2016**, *115*, 273–283. [CrossRef]
33. Wongkeo, W.; Thongsanitgarn, P.; Pimraksa, K.; Chaipanich, A. Compressive Strength, Flexural Strength and Thermal Conductivity of Autoclaved Concrete Block Made Using Bottom Ash as Cement Replacement Materials. *Mater. Des.* **2012**, *35*, 434–439. [CrossRef]
34. Cai, L.; Li, X.; Liu, W.; Ma, B.; Lv, Y. The Slurry and Physical-Mechanical Performance of Autoclaved Aerated Concrete with High Content Solid Wastes: Effect of Grinding Process. *Constr. Build. Mater.* **2019**, *218*, 28–39. [CrossRef]
35. Amaral, L.F.; Oliveira, I.R.; Salomão, R.; Frollini, E.; Pandolfelli, V.C. Temperature and Common-Ion Effect on Magnesium Oxide (MgO) Hydration. *Ceram. Int.* **2010**, *36*, 1047–1054. [CrossRef]
36. Martín-Sedeño, M.C.; Cuberos, A.J.M.; de la Torre, Á.G.; Álvarez-Pinazo, G.; Ordónez, L.M.; Gateshki, M.; Aranda, M.A.G. Aluminum-Rich Belite Sulfoaluminate Cements: Clinkering and Early Age Hydration. *Cem. Concr. Res.* **2010**, *40*, 359–369. [CrossRef]
37. Londono-Zuluaga, D.; Tobón, J.I.; Aranda, M.A.G.; Santacruz, I.; de la Torre, A.G. Clinkering and Hydration of Belite-Alite-Ye'elimite Cement. *Cem. Concr. Compos.* **2017**, *80*, 333–341. [CrossRef]
38. Klimesch, D.S.; Ray, A.; Guerbois, J.-P. Differential Scanning Calorimetry Evaluation of Autoclaved Cement Based Building Materials Made with Construction and Demolition Waste. *Thermochim. Acta* **2002**, *389*, 195–198. [CrossRef]
39. Baquerizo, L.G.; Matschei, T.; Scrivener, K.L. Impact of Water Activity on the Stability of Ettringite. *Cem. Concr. Res.* **2016**, *79*, 31–44. [CrossRef]
40. Baquerizo, L.G.; Matschei, T.; Scrivener, K.L.; Saeidpour, M.; Thorell, A.; Wadsö, L. Methods to Determine Hydration States of Minerals and Cement Hydrates. *Cem. Concr. Res.* **2014**, *65*, 85–95. [CrossRef]
41. Matsui, K.; Kikuma, J.; Tsunashima, M.; Ishikawa, T.; Matsuno, S.Y.; Ogawa, A.; Sato, M. In Situ Time-Resolved X-ray Diffraction of Tobermorite Formation in Autoclaved Aerated Concrete: Influence of Silica Source Reactivity and Al Addition. *Cem. Concr. Res.* **2011**, *41*, 510–519. [CrossRef]